PHYSICAL REVIEW B **91**, 224306 (2015)

Lattice vibrations in the Frenkel-Kontorova Model. II. Thermal conductivity

Qingping Meng,[*] Lijun Wu, David O. Welch, and Yimei Zhu[†]
Brookhaven National Laboratory, Upton, New York 11973, USA

(Received 22 December 2014; revised manuscript received 1 June 2015; published 17 June 2015)

We applied the formulas for the phonon spectral-density function that we presented in the previous paper of this series to analyze the thermal conductivity of the lattice in the framework of the Frenkel-Kontorova (FK) model. We found that two extra mechanisms of phonon scattering (different from the point impurities, three-phonon processes, and boundary scattering typical of all crystals), viz., resonance, and anharmonic scattering, that mainly influences the thermal conductivity of the lattice. The frequencies of resonance scattering are discrete, and their number increases from a finite number to infinity with their transition from the commensurate to the incommensurate state. Changing the amplitude and period of the FK model changes the frequencies and the frequency number of resonance scattering and the intensity of anharmonic scattering. We analyze these changes in detail. Our theory can explain all existing numerical results on this problem and suggest strategies to reduce the thermal conductivity of the lattice of layered materials.

DOI: 10.1103/PhysRevB.91.224306 PACS number(s): 63.20.D−, 63.70.+h

I. INTRODUCTION

In the first paper of this series [1], termed number I, we derived general expressions for vibrational properties of the lattice of the Frenkel-Kontorova (FK) model, number density, and the energy of the system. These derivations utilized the technique of thermodynamic Green's functions, based on quantum field-theoretic methods.

In layered materials with two interpenetrating sublattices, we can simply use an on-site potential to describe their atomic interactions. The FK model that describes the effects of a typical on-site potential has been studied extensively [2]. As we mentioned in the Introduction to paper I, one of our motivations for studying this system was that very low lattice thermal conductivity was found experimentally for some materials consisting of two interpenetrating incommensurate sublattices, such as Na_xCoO_2 [3], $Ca_3Co_4O_9$ [4,5], and $Bi_{2-x}Pb_xSr_2Co_2O_y$ [5,6]. Therefore, these materials probably have good thermoelectric properties [7]. In another recent paper, we discussed the mechanism underlying the low lattice thermal conductivity in $Ca_3Co_4O_9$, based on fitting it to experimental data, using Callaway's phenomenological theory [8]. Furthermore, our experimental results yielded some clues as to the origin of this low thermal conductivity and suggested qualitative explanations [8]; nevertheless, a systematic theoretical description still is lacking.

Some numerical simulations [9–16] of thermal conductivity with an on-site potential previously were carried out. Although they yielded some useful results, showing that the thermal conductivity of a one-dimensional lattice diverges with the system's size [10–15] and that the thermal conductivity for an anharmonic on-site potential [16,17] tends monotonically to zero with increasing temperature, the mechanisms of thermal conductivity were only those conjectured from these numerical simulations. Therefore, having an analytical solution to complement those numerical studies is highly desirable.

In this paper, we use the Green's functions deduced in paper I to calculate the correlation function of the energy-flow operator [18] and then to obtain analytical formulas of thermal conductivity for the FK model with various periods; these, in turn, led to various-order commensurate states and to an incommensurate state that we derived, based on the Kubo formula for thermal conductivity. Utilizing these analytical formulas, we analyzed in detail the mechanism of thermal conductivity for the FK model.

II. GENERAL FORMALISM OF LATTICE THERMAL CONDUCTIVITY

The lattice thermal conductivity from the Kubo expression is

$$\kappa = \lim_{\delta\to 0} \frac{k_B\beta}{V}\int_0^\infty dt\, e^{-\delta t}\int_0^\beta d\lambda \langle S(0)S(t+i\hbar\lambda)\rangle, \tag{2.1}$$

where V is the volume of the crystal, $\beta = \frac{1}{k_BT}$, T is temperature, and $S(t)$ is the energy-flow operator of the lattice at time t. Ignoring the nondiagonal parts of the energy-flow operator, the energy-flow operator is [18]

$$S(t) = \sum_k \hbar\omega_k v_k n_k, \tag{2.2}$$

where ω_k is the frequency of the normal mode with wave vector k of the unperturbed crystal, v_k is the group velocity, and $n_k = a_k^+ a_k$ is the number-density operator of the phonon. From Eq. (2.2), thermal conductivity then is written as

$$\kappa = \lim_{\delta\to 0}\frac{k_B\beta\hbar^2}{V}\sum_{kq} v_k v_q \omega_k \omega_q \int_0^\infty dt e^{-\delta t} \times \int_0^\beta d\lambda F_{kq}(t+i\hbar\lambda). \tag{2.3}$$

The correlation function $F_{kq}(t)$ is

$$F_{kq}(t) = \langle n_k(0)n_q(t)\rangle = \langle a_k^+(0)a_k(0)a_q^+(t)a_q(t)\rangle \approx \langle a_k^+(0)a_q(t)\rangle\langle a_k(0)a_q^+(t)\rangle. \tag{2.4}$$

---

[*] Corresponding author: qmeng@bnl.gov

[†] Corresponding author: zhu@bnl.gov

We used the decoupled relation [19] $\langle abcd\rangle = \langle ab\rangle\langle cd\rangle + \langle ac\rangle\langle bd\rangle + \langle ad\rangle\langle bc\rangle$ and ignored those terms involving two creation and two annihilation operators because they are negligibly small; furthermore, we ignored the correlation function with same time argument since only such correlation functions with different times contribute to thermal conductivity.

Combining Eqs. (2.13a) and (2.13b) in paper I and Eqs. (2.1)–(2.4), we obtained the following equation for the thermal conductivity of the lattice:

$$\kappa = \frac{\pi k_B \beta^2 \hbar^2}{16V} \sum_{kq} v_k v_q \omega_k \omega_q \int_{-\infty}^{\infty} d\omega \times \left(1 + \frac{\omega}{\omega_q} + \frac{\omega}{\omega_k} + \frac{\omega^2}{\omega_k \omega_q}\right)^2 J_{kq}(\omega) J_{qk}(\omega) e^{\beta\hbar\omega}, \tag{2.5}$$

where $J_{kq}(\omega)$ is the spectral-density function defined in paper I. Equation (2.5) is the starting point for our calculation of the lattice's thermal conductivity.

III. APPLICATIONS

Next, we examined the properties of phonon transport for various different degrees of matching between the unit-cell sizes a and b of the two sublattices of the FK model.

A. $a = b$

Here, the period of the FK model equals that of the lattice chain. The spectral-density function (as detailed in paper I) is

$$J_{kq}(\omega) = \frac{\delta_{qk}\omega_k}{\tilde{\omega}_k^{(1)}} \frac{\delta\left(\omega - \tilde{\omega}_k^{(1)}\right) - \delta\left(\omega + \tilde{\omega}_k^{(1)}\right)}{e^{\beta\hbar\omega} - 1}, \tag{3.1}$$

where $\tilde{\omega}_k^{(1)} = (\omega_k^2 + M_1)^{1/2}$ and M_1 is given in Eq. (3.4) of paper I. Substituting and integrating Eq. (3.1) into Eq. (2.5), we obtain the result that herein thermal conductivity is infinite, viz., consistent with the results of many numerical simulations [10–17]. Because our system here is an infinite lattice chain, thermal conductivity diverges as $N \to \infty$ in numerical simulations.

B. $a = \frac{b}{2}$

In paper I, we show that we can write the spectral-density function in this case as follows:

$$J_{kq} = \frac{2M_2\Gamma_{q+(\pi/a)}}{\pi(e^{\beta\hbar\omega} - 1)} \frac{\delta_{qk}\omega_q M_2 + \delta_{q+(\pi/a)k}(\omega_q \omega_{q+(\pi/a)})^{1/2}\left(\omega^2 - \omega_q^2\right)}{\left[\omega^2 - \left(\tilde{\omega}_k^{(2)}\right)^2\right]^2 + \Gamma_{q+(\pi/a)^2} M_2^4}, \tag{3.2}$$

where $\tilde{\omega}_k^{(2)} = (\omega_k^2 + M_2^2 \Delta_{k+(\pi/a)})^{1/2}$ and $\Delta_{k+(\pi/a)}$, $\Gamma_{q+(\pi/a)}$, and M_2 are defined in paper I. From the spectral-density function, we can consider contributions to thermal conductivity in two cases.

Case 1. $k = q$.

In this case, the spectral-density function becomes

$$J_{kk} = \frac{2\omega_k M_2^2 \Gamma_{k+(\pi/a)}}{\pi(e^{\beta\hbar\omega} - 1)} \frac{1}{\left[\omega^2 - \left(\tilde{\omega}_k^{(2)}\right)^2\right]^2 + \Gamma_{q+(\pi/a)^2} M_2^4}, \tag{3.3}$$

and the contributions of these phonons to the thermal conductivity is

$$\kappa_{k=q} = \frac{k_B \beta^2 \hbar^2}{4\pi V} \sum_q v_q^2 \omega_q^4 \int_{-\infty}^{\infty} d\omega \left(1 + \frac{\omega}{\omega_q}\right)^4 \frac{e^{\beta\hbar\omega}}{(e^{\beta\hbar\omega} - 1)^2} \frac{\Gamma_{q+(\pi/a)^2} M_2^4}{\left\{\left[\omega^2 - \left(\tilde{\omega}_q^{(2)}\right)^2\right]^2 + \Gamma_{q+(\pi/a)^2} M_2^4\right\}^2}. \tag{3.4}$$

Case 2. $k = q + \frac{\pi}{a}$,

$$J_{q+(\pi/a)q} = \frac{2M_2\Gamma_{q+(\pi/a)}}{\pi(e^{\beta\hbar\omega} - 1)} \frac{(\omega_q \omega_{q+(\pi/a)})^{1/2}\left(\omega^2 - \omega_q^2\right)}{\left[\omega^2 - \left(\tilde{\omega}_q^{(2)}\right)^2\right]^2 + \Gamma_{q+(\pi/a)^2} M_2^4}, \tag{3.5a}$$

and

$$J_{qq+(\pi/a)} = \frac{2M_2\Gamma_q}{\pi(e^{\beta\hbar\omega} - 1)} \frac{(\omega_q \omega_{q+(\pi/a)})^{1/2}\left(\omega^2 - \omega_{q+(\pi/a)}^2\right)}{\left[\omega^2 - \left(\tilde{\omega}_{q+(\pi/a)}^{(2)}\right)^2\right]^2 + \Gamma_q^2 M_2^4}. \tag{3.5b}$$

The thermal conductivity is

$$\kappa_{k=q+(\pi/a)} = \frac{k_B \beta^2 \hbar^2}{4\pi V} \sum_q v_q v_{q+(\pi/a)} (\omega_q \omega_{q+(\pi/a)})^2 \int_{-\infty}^{\infty} d\omega \left(1 + \frac{\omega}{\omega_q} + \frac{\omega}{\omega_{q+(\pi/a)}} + \frac{\omega^2}{\omega_q \omega_{q+(\pi/a)}}\right)^2 \frac{e^{\beta\hbar\omega}}{(e^{\beta\hbar\omega} - 1)^2} \times \frac{M_2^2 \Gamma_q \Gamma_{q+(\pi/a)}\left(\omega^2 - \omega_q^2\right)\left(\omega^2 - \omega_{q+(\pi/a)}^2\right)}{\left\{\left[\omega^2 - \left(\tilde{\omega}_q^{(2)}\right)^2\right]^2 + \Gamma_{q+(\pi/a)^2} M_2^4\right\}\left\{\left[\omega^2 - \left(\tilde{\omega}_{q+(\pi/a)}^{(2)}\right)^2\right]^2 + \Gamma_q^2 M_2^4\right\}}. \tag{3.6}$$

For small values of $\Gamma_{k+(\pi/a)}$ and Γ_k that are related to the width at half maximum of the peak in the energy distribution, the integrands in Eqs. (3.4) and (3.6) peak around $\omega = \tilde{\omega}_q^{(2)}$ and $\omega = \tilde{\omega}_q^{(2)} = \tilde{\omega}_{q+(\pi/a)}^{(2)}$. We can evaluate these integrals analytically by replacing the peak distribution by a Dirac function. We then obtain the total thermal conductivity as

$$\begin{aligned}\kappa &= \frac{k_B\beta^2\hbar^2}{8VM_2^2}\sum_q \frac{e^{\beta\hbar\tilde{\omega}_q^{(2)}}}{\left(e^{\beta\hbar\tilde{\omega}_q^{(2)}}-1\right)^2}\left[1+6\left(\frac{\tilde{\omega}_q^{(2)}}{\omega_q}\right)^2+\left(\frac{\tilde{\omega}_q^{(2)}}{\omega_q}\right)^4\right]\frac{v_q^2\omega_q^4}{\tilde{\omega}_q^{(2)}\Gamma_{q+(\pi/a)}}\\ &\quad+\frac{k_B\beta^2\hbar^2}{4VM_2^4}\sum_q{}' \frac{e^{\beta\hbar\tilde{\omega}_q^{(2)}}}{\left(e^{\beta\hbar\tilde{\omega}_q^{(2)}}-1\right)^2}\left[\left(1+\frac{\left(\tilde{\omega}_q^{(2)}\right)^2}{\omega_q\omega_{q+(\pi/a)}}\right)^2+\left(\frac{\tilde{\omega}_q^{(2)}}{\omega_q}+\frac{\tilde{\omega}_q^{(2)}}{\omega_{q+(\pi/a)}}\right)^2\right]\\ &\quad\times\frac{v_qv_{q+(\pi/a)}(\omega_q\omega_{q+(\pi/a)})^2\left[\left(\tilde{\omega}_q^{(2)}\right)^2-\omega_q^2\right]\left[\left(\tilde{\omega}_q^{(2)}\right)^2-\omega_{q+(\pi/a)^2}\right]}{\tilde{\omega}_q^{(2)}(\Gamma_q+\Gamma_{q+(\pi/a)})}. \end{aligned} \tag{3.7}$$

Equation (3.7) is the familiar relaxation-time expression. The first term therein is the contribution from $k = q$. In this case, the reciprocal of the phonon lifetime in the FK potential is $\tau^{-1} \propto \frac{\Gamma_{q+(\pi/a)}M_2^2\tilde{\omega}_q^{(2)}}{\omega_q^2}$. Using Eq. (3.27b) from paper I, we can write the reciprocal of the phonon lifetime as

$$\begin{aligned}\tau^{-1} &\propto \frac{\pi M_2^2\tilde{\omega}_q^{(2)}}{2|\omega_{q+(\pi/a)}|\omega_q^2}\left[\delta\left(\tilde{\omega}_q^{(2)}-\omega_{q+(\pi/a)}\right)\right.\\ &\quad\left.+\,\delta\left(\tilde{\omega}_q^{(2)}+\omega_{q+(\pi/a)}\right)\right].\end{aligned} \tag{3.8}$$

Equation (3.8) reveals that there is resonance scattering at a frequency that is the solution for $\tilde{\omega}_q^{(2)} = |\omega_{q+(\pi/a)}|$. Figure 1 is a schematic illustrating how to assess the resonance frequency. In the calculation of Fig. 1, we let the largest frequency of the unperturbed normal mode be $\omega_L = 1$ [1]. In this figure, the points corresponding to the addition sign meet $\tilde{\omega}_q^{(2)} = |\omega_{q+(\pi/a)}|$. There are two solutions for this equation in Fig. 1. When the frequency of an incident phonon is a resonance frequency, the phonon lifetime is zero, meaning that the phonon is local only, and cannot propagate.

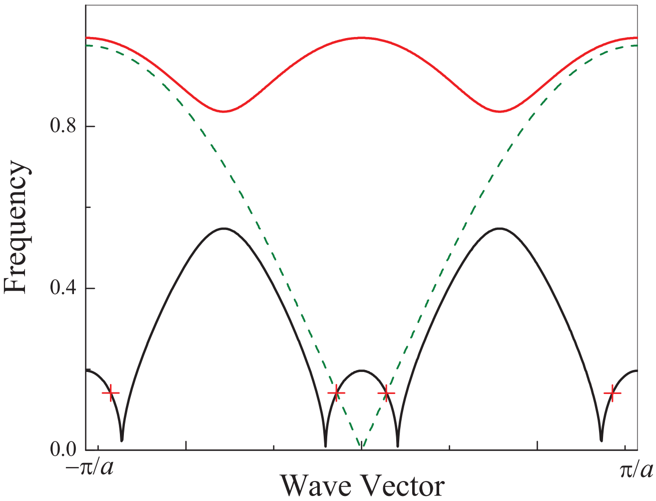

FIG. 1. (Color online) Schematic illustrating how to calculate resonance frequency for $a = \frac{b}{2}$. The green dashed line is ω_q, and the black and red solid lines show the two branches of $\tilde{\omega}_q^{(2)}$. The red points shown by addition signs satisfy $\tilde{\omega}_q^{(2)} = |\omega_q|$ or $\tilde{\omega}_q^{(2)} = |\omega_{q+(\pi/a)}|$. The corresponding frequencies of these points are resonant ones. $\omega_L = 1$ and $\frac{\pi^2V_0}{ma^2} = 0.1$ are used in the calculation.

The second term in Eq. (3.7) is the contribution from $k = q + \frac{\pi}{a}$. The prime symbol represents a sum for the value of q for $\tilde{\omega}_q^{(2)} = \tilde{\omega}_{q+(\pi/a)}^{(2)}$; it is not a strict condition here because the period of $\tilde{\omega}_q^{(2)}$ is $\frac{\pi}{a}$. The phonon's lifetime is

$$\begin{aligned}\tau^{-1} &\propto \frac{M_2^4\tilde{\omega}_q^{(2)}}{\omega_q\omega_{q+(\pi/a)}\left[\left(\tilde{\omega}_q^{(2)}\right)^2-\omega_q^2\right]\left[\left(\tilde{\omega}_q^{(2)}\right)^2-\omega_{q+(\pi/a)^2}\right]}\\ &\quad\times\left[\frac{\delta\left[\left(\tilde{\omega}_q^{(2)}\right)^2-\omega_q^2\right]}{|\omega_q|}+\frac{\delta\left[\left(\tilde{\omega}_q^{(2)}\right)^2-\omega_{q+(\pi/a)^2}\right]}{|\omega_{q+(\pi/a)}|}\right].\end{aligned} \tag{3.9}$$

Equation (3.9) also details the phonon's resonance scattering. The resonance frequency is obtained from

$$\tilde{\omega}_q^{(2)} = |\omega_{q+(\pi/a)}| \quad\text{and}\quad \tilde{\omega}_q^{(2)} = |\omega_q|. \tag{3.10}$$

From Eqs. (3.8) and (3.9), we find that the phonons described by a special frequency are scattered completely, implying that these special frequency phonons do not contribute to thermal conductivity. However, the transport of other phonons occurs without resistance; therefore, the total thermal conductivity still is infinite even if other mechanisms, such as point impurities, three-phonon processes, and the boundary scattering of thermal conductivity, are not considered.

C. $a = \frac{b}{3}$

For this case, we first consider the contribution of $C_2(k_1,k_2)$ (see paper I). The spectral-density function is

$$J_{kq} = \frac{2}{e^{\beta\hbar\omega} - 1} \times \frac{\left(\frac{\delta_{qk}}{\pi}\omega_q + \varphi_{q+(2\pi/3a)}\Delta_{q+(2\pi/3a)} + \varphi_{q-(2\pi/3a)}\Delta_{q-(2\pi/3a)}\right)\left(\phi_{q+(2\pi/3a)}\Gamma_{q+(2\pi/3a)} + \phi_{q-(2\pi/3a)}\Gamma_{q-(2\pi/3a)}\right) - \left[\omega^2 - \left(\tilde{\omega}_q^{(3)}\right)^2\right]\left(\varphi_{q+(2\pi/3a)}\Gamma_{q+(2\pi/3a)} + \varphi_{q-(2\pi/3a)}\Gamma_{q-(2\pi/3a)}\right)}{\left[\omega^2 - \left(\tilde{\omega}_q^{(3)}\right)^2\right]^2 + \left(\phi_{q+(2\pi/3a)}\Gamma_{q+(2\pi/3a)} + \phi_{q-(2\pi/3a)}\Gamma_{q-(2\pi/3a)}\right)^2}, \tag{3.11}$$

where φ_q, ϕ_q, and $\tilde{\omega}_q^{(3)}$ are defined in paper I. Using the same method as used in the section above, we obtain the contribution to thermal conductivity for several cases:

Case 1. $k = q$,

$$\kappa_{k=q} = \frac{k_B\beta^2\hbar^2}{8V}\sum_q \frac{e^{\beta\hbar\tilde{\omega}_q^{(3)}}}{\left(e^{\beta\hbar\tilde{\omega}_q^{(3)}} - 1\right)^2}\left[1 + 6\left(\frac{\tilde{\omega}_q^{(3)}}{\omega_q}\right)^2 + \left(\frac{\tilde{\omega}_q^{(3)}}{\omega_q}\right)^4\right]\frac{v_q^2\omega_q^4}{\tilde{\omega}_q^{(3)}}\frac{\left(1 - \frac{\alpha_2^2(\Delta_{q+(2\pi/3a)} - \Delta_{q-(2\pi/3a)})}{\omega_{q+(2\pi/3a)2} - \omega_{q-(2\pi/3a)2}}\right)^2}{|\phi_{q+(2\pi/3a)}\Gamma_{q+(2\pi/3a)} + \phi_{q-(2\pi/3a)}\Gamma_{q-(2\pi/3a)}|}. \tag{3.12}$$

Case 2. $k = q + \frac{2\pi}{3a}$,

$$\kappa_{k=q+(2\pi/3a)} = \frac{k_B\beta^2\hbar^2}{8V}{\sum_q}' \frac{e^{\beta\hbar\tilde{\omega}_q^{(3)}}}{\left(e^{\beta\hbar\tilde{\omega}_q^{(3)}} - 1\right)^2}\left[\left(1 + \frac{\left(\tilde{\omega}_k^{(3)}\right)^2}{\omega_k\omega_{k+(2\pi/3a)}}\right)^2 + \left(\frac{\tilde{\omega}_k^{(3)}}{\omega_k} + \frac{\tilde{\omega}_k^{(3)}}{\omega_{k+(2\pi/3a)}}\right)^2\right] \times \frac{v_q^2\omega_q^4\alpha_2^2}{\tilde{\omega}_q^{(3)}}\frac{\left(\Delta_q + \frac{\alpha_2(\Delta_q - \Delta_{q-(2\pi/3a)})}{\omega_q^2 - \omega_{q-(2\pi/3a)2}}\right)^2}{|\phi_q\Gamma_q + \phi_{q-(2\pi/3a)}\Gamma_{q-(2\pi/3a)}|}. \tag{3.13}$$

Case 3. $k = q - \frac{2\pi}{3a}$,

$$\kappa_{k=q-(2\pi/3a)} = \frac{k_B\beta^2\hbar^2}{8V}{\sum_q}' \frac{e^{\beta\hbar\tilde{\omega}_q^{(3)}}}{\left(e^{\beta\hbar\tilde{\omega}_q^{(3)}} - 1\right)^2}\left[\left(1 + \frac{\left(\tilde{\omega}_k^{(3)}\right)^2}{\omega_k\omega_{k-(2\pi/3a)}}\right)^2 + \left(\frac{\tilde{\omega}_k^{(3)}}{\omega_k} + \frac{\tilde{\omega}_k^{(3)}}{\omega_{k-(2\pi/3a)}}\right)^2\right] \times \frac{v_q^2\omega_q^4\alpha_2^2}{\tilde{\omega}_q^{(3)}}\frac{\left(\Delta_q + \frac{\alpha_2(\Delta_q - \Delta_{q+(2\pi/3a)})}{\omega_q^2 - \omega_{q+(2\pi/3a)2}}\right)^2}{|\phi_q\Gamma_q + \phi_{q+(2\pi/3a)}\Gamma_{q+(2\pi/3a)}|}. \tag{3.14}$$

The prime symbol in Eqs. (3.13) and (3.14) represents only the sum for q of $\tilde{\omega}_q^{(3)} = \tilde{\omega}_{q+(2\pi/\beta a)}^{(3)}$ [Eq. (3.13)] and $\tilde{\omega}_q^{(3)} = \tilde{\omega}_{q-(2\pi/\beta a)}^{(3)}$ [Eq. (3.14)]. The thermal conductivities from Eqs. (3.12)–(3.14) are similar to the result of $a = \frac{b}{2}$, i.e., resonance scattering in some frequencies will result in zero thermal conductivity, whereas phonons with other frequencies have resistance-free transport provided that point impurities, three-phonon processes, and boundary scattering are not considered in calculating the lattice thermal conductivity. The resonance frequency is obtained from one of the following three equations:

$$\tilde{\omega}_q^{(3)} = |\omega_{q+(2\pi/3a)}|, \tag{3.15a}$$

$$\tilde{\omega}_q^{(3)} = |\omega_{q-(2\pi/3a)}|, \tag{3.15b}$$

and

$$\tilde{\omega}_q^{(3)} = |\omega_q|. \tag{3.15c}$$

For a structure higher than a second-order commensurate one, the effect of $C_3(k_1,k_2,k_3)$ does not disappear (see paper I). When the effects of $C_3(k_1,k_2,k_3)$ and $C_4(k_1,k_2,k_3,k_4)$ are considered, we obtain the spectral-density function,

$$J_{kq} = \frac{2}{\exp(\beta\hbar\omega) - 1}\frac{\left(\frac{\delta_{qk}}{\pi}\omega_q + \mathrm{Re}\,\xi\right)\mathrm{Im}\,\zeta - \left[\omega^2 - \left(\tilde{\omega}_q^{(3)}\right)^2\right]\mathrm{Im}\,\xi}{\left[\omega^2 - \left(\tilde{\omega}_q^{(3)}\right)^2\right]^2 + (\mathrm{Im}\,\zeta)^2}, \tag{3.16}$$

where $(\tilde{\omega}_q^{(3)})^2 = \omega_q^2 - \mathrm{Re}\,\zeta$. ξ and ζ are two functions dependent on the vectors k and q. "Re" and "Im," respectively, represent their real and imaginary parts. Details are given in the Supplemental Material of paper I. The thermal conductivities for three cases are the following:

Case 1. $q = k$,

$$\kappa_{q=k} = \frac{k_B\beta^2\hbar^2}{4V}\sum_k \frac{\exp\left(\beta\hbar\tilde{\omega}_k^{(3)}\right)}{\left[\exp\left(\beta\hbar\tilde{\omega}_k^{(3)}\right) - 1\right]^2}\left[1 + 6\left(\frac{\tilde{\omega}_k^{(3)}}{\omega_k}\right)^2 + \left(\frac{\tilde{\omega}_k^{(3)}}{\omega_k}\right)^4\right]\frac{v_k^2\omega_k^2[\omega_k + \pi(\mathrm{Re}\,\xi)_{q=k}]^2}{\tilde{\omega}_k^{(3)}|(\mathrm{Im}\,\zeta)_{q=k}|}. \tag{3.17}$$

Case 2. $q = k + \frac{2\pi}{3a}$,

$$\kappa_{q=k+(2\pi/3a)} = \frac{k_B\beta^2\hbar^2}{2V}\sum_k{}' \frac{(\alpha_2+\alpha_4)^2\exp\left(\beta\hbar\tilde{\omega}_k^{(3)}\right)}{\left[\exp\left(\beta\hbar\tilde{\omega}_k^{(3)}\right)-1\right]^2}\left[\left(1+\frac{\left(\tilde{\omega}_k^{(3)}\right)^2}{\omega_k\omega_{k+(2\pi/3a)}}\right)^2+\left(\frac{\tilde{\omega}_k^{(3)}}{\omega_k}+\frac{\tilde{\omega}_k^{(3)}}{\omega_{k+(2\pi/3a)}}\right)^2\right] \times \frac{v_k v_{k+(2\pi/3a)}(\omega_k\omega_{k+(2\pi/3a)})^2\Delta_k\Delta_{k+(2\pi/3a)}}{\tilde{\omega}_k^{(3)}|(\mathrm{Im}\,\zeta)_1+(\mathrm{Im}\,\zeta)_2|}. \tag{3.18}$$

Case 3. $q = k - \frac{2\pi}{3a}$,

$$\kappa_{q=k-(2\pi/3a)} = \frac{k_B\beta^2\hbar^2}{2V}\sum_k{}' \frac{(\alpha_2+\alpha_4)^2\exp\left(\beta\hbar\tilde{\omega}_k^{(3)}\right)}{\left[\exp\left(\beta\hbar\tilde{\omega}_k^{(3)}\right)-1\right]^2}\left[\left(1+\frac{\left(\tilde{\omega}_k^{(3)}\right)^2}{\omega_k\omega_{k-(2\pi/3a)}}\right)^2+\left(\frac{\tilde{\omega}_k^{(3)}}{\omega_k}+\frac{\tilde{\omega}_k^{(3)}}{\omega_{k-(2\pi/3a)}}\right)^2\right] \times \frac{v_k v_{k-(2\pi/3a)}(\omega_k\omega_{k-(2\pi/3a)})^2\Delta_k\Delta_{k-(2\pi/3a)}}{\tilde{\omega}_k^{(3)}|(\mathrm{Im}\,\zeta)_3+(\mathrm{Im}\,\zeta)_4|}, \tag{3.19}$$

where $(\mathrm{Im}\,\zeta)_1$, $(\mathrm{Im}\,\zeta)_2$, $(\mathrm{Im}\,\zeta)_3$, and $(\mathrm{Im}\,\zeta)_4$ are $\mathrm{Im}\,\zeta$ after using the $k + \frac{2\pi}{3a} \to q$, $k \to k$; $k + \frac{2\pi}{3a} \to k$, $k \to q$; $k - \frac{2\pi}{3a} \to q$, $k \to k$; and $k - \frac{2\pi}{3a} \to k$, $k \to q$ transitions, respectively. Carefully analyzing $\mathrm{Im}\,\zeta$ in the Supplemental Material of paper I, we find that not only can the quadratic and quartic terms [the first term of Eq. (S.60) in the Supplemental Material of paper I] can bring about resonance scattering, but also the cubic term can [i.e., the second and third terms of Eq. (S.60)] from the FK on-site potential. We can assess the resonance frequencies by solving one of the equations of Eq. (3.15). Moreover, we note that the cubic term also results in other anharmonic scatterings [the last six terms of Eq. (S.60) in the Supplemental Material of paper I], i.e., the cubic term of the FK on-site potential implies result that resonance scattering is not the only source of phonon scattering. Anharmonic scattering, unlike resonance scattering, will scatter phonons of all frequencies. Therefore, when such scattering is considered, the total thermal conductivity will be finite, i.e., the divergence of thermal conductivity with the system's size will be lacking. This result is consistent with some numerical experiments [16,17]. As indicated in paper I, when the cubic term from the FK on-site potential is considered, a theoretical solution becomes impossible for higher-order commensurate states. However, from assessing the third-order commensurate state, we find that the cubic term mainly leads to anharmonic scattering of all frequency phonons, although the phonon lifetime for scattering has a finite value. The anharmonic contribution is similar to that obtained before [20–22]. Therefore, in subsequent sections, we only consider the effect of the quadratic term.

D. $a = s_r b$

The wave vector of the periodic FK model is $g = \frac{2\pi s_r}{a}$ for any order of commensurate state. The spectral-density function is

$$J_{kq} = -\frac{2}{\pi[\exp(\beta\hbar\omega)-1]} \times \frac{\alpha^2\mathrm{Im}\left(\theta_1^{(r)}+\theta_2^{(r)}\right)\left\{\delta_{qk}\omega_q+\mathrm{Re}\left[\alpha\eta_1^{(r)}+\alpha^2\left(\eta_2^{(r)}-\eta_3^{(r)}\right)\right]\right\}+\left[\omega^2-\left(\tilde{\omega}_q^{(r)}\right)^2\right]\mathrm{Im}\left[\alpha\eta_1^{(r)}+\alpha^2\left(\eta_2^{(r)}-\eta_3^{(r)}\right)\right]}{\left[\omega^2-\left(\tilde{\omega}_q^{(r)}\right)^2\right]^2+\alpha^4\left[\mathrm{Im}\left(\theta_1^{(r)}+\theta_2^{(r)}\right)\right]^2}, \tag{3.20}$$

where $(\tilde{\omega}_q^{(r)})^2 = \omega_q^2 + \alpha^2\mathrm{Re}(\theta_1^{(r)}+\theta_2^{(r)})$. α, $\theta_1^{(r)}$, $\theta_2^{(r)}$, $\eta_1^{(r)}$, $\eta_2^{(r)}$, and $\eta_3^{(r)}$ are defined in paper I. The lattice-thermal conductivities in various cases are the following:

Case 1. $k = q$.

When $k = q$, $\eta_1^{(r)}$ and $\eta_2^{(r)}$ disappear. From Eq. (2.5), we have

$$\kappa_{k=q} = \frac{k_B\beta^2\hbar^2}{8V\alpha^2}\sum_k \frac{e^{\beta\hbar\tilde{\omega}_k^{(r)}}}{\left(e^{\beta\hbar\tilde{\omega}_k^{(r)}}-1\right)^2}\left[1+6\left(\frac{\tilde{\omega}_k^{(r)}}{\omega_k}\right)^2+\left(\frac{\tilde{\omega}_k^{(r)}}{\omega_k}\right)^4\right]\frac{v_k^2\omega_k^4}{\tilde{\omega}_k^{(r)}}\frac{\left(1-\frac{\alpha^2}{\omega_k}\mathrm{Re}\,\eta_3^{(r)}\right)^2}{\left|\mathrm{Im}\left(\theta_1^{(r)}+\theta_2^{(r)}\right)\right|}. \tag{3.21}$$

Case 2. $k = q - g$.

We first need to know the values of J_{q-gq} and J_{qq-g}, respectively, that are obtained from J_{kq} by substituting the subscripts $k \to q - g, q \to q$, and $k \to q, q \to q - g$. Then, $\eta_2^{(r)}$ and $\eta_3^{(r)}$ disappear, and $\eta_1^{(r)}$ becomes

$$\eta_1^{(r)} = (\omega_q\omega_{q-g})^{1/2}(\Delta_{q-g} - i\Gamma_{q-g}) \tag{3.22a}$$

for the substitution of subscripts $k \to q-g, q \to q$, and

$$\eta_1^{(r)} = (\omega_{q-g}\omega_q)^{1/2}(\Delta_q - i\Gamma_q) \tag{3.22b}$$

for the substitution of subscripts $k \to q, q \to q-g$. Other terms, such as $\theta_1^{(r)}$, $\theta_2^{(r)}$, and $\tilde{\omega}_q^{(r)}$, are similar to $\eta_1^{(r)}$, and then, we have

$$J_{q-gq} = -\frac{2}{\pi[\exp(\beta\hbar\omega)-1]}\left\{\frac{\alpha^3\mathrm{Im}\big(\theta_1^{(r)}+\theta_2^{(r)}\big)\mathrm{Re}\big(\eta_1^{(r)}\big)+\alpha\big[\omega^2-\big(\tilde{\omega}_q^{(r)}\big)^2\big]\mathrm{Im}\big(\eta_1^{(r)}\big)}{\big[\omega^2-\big(\tilde{\omega}_q^{(r)}\big)^2\big]^2+\alpha^4\big[\mathrm{Im}\big(\theta_1^{(r)}+\theta_2^{(r)}\big)\big]^2}\right\}_{k\to q-g, q\to q}, \tag{3.23a}$$

$$J_{qq-g} = -\frac{2}{\pi[\exp(\beta\hbar\omega)-1]}\left\{\frac{\alpha^3\mathrm{Im}\big(\theta_1^{(r)}+\theta_2^{(r)}\big)\mathrm{Re}\big(\eta_1^{(r)}\big)+\alpha\big[\omega^2-\big(\tilde{\omega}_q^{(r)}\big)^2\big]\mathrm{Im}\big(\eta_1^{(r)}\big)}{\big[\omega^2-\big(\tilde{\omega}_q^{(r)}\big)^2\big]^2+\alpha^4\big[\mathrm{Im}\big(\theta_1^{(r)}+\theta_2^{(r)}\big)\big]^2}\right\}_{k\to q, q\to q-g}. \tag{3.23b}$$

The thermal conductivity is

$$\kappa_{k=q-g} = \frac{k_B\beta^2\hbar^2}{4V}\sum_q{}' \frac{e^{\beta\hbar\tilde{\omega}_q^{(r)}}}{\big(e^{\beta\hbar\tilde{\omega}_q^{(r)}}-1\big)^2}\frac{v_q v_{q-g}\omega_q^2\omega_{q-g}^2\Delta_q\Delta_{q-g}\big[\big(\frac{\tilde{\omega}_q^{(r)}}{\omega_q}+\frac{\tilde{\omega}_q^{(r)}}{\omega_{q-g}}\big)^2+\big(\frac{(\tilde{\omega}_q^{(r)})^2}{\omega_q\omega_{q-g}}+1\big)^2\big]}{\tilde{\omega}_q^{(r)}\big[\big|\mathrm{Im}\big(\theta_1^{(r)}+\theta_2^{(r)}\big)\big|_{q\to q}+\big|\mathrm{Im}\big(\theta_1^{(r)}+\theta_2^{(r)}\big)\big|_{q\to q-g}\big]}. \tag{3.24}$$

Case 3. $k = q + g$.

Similar to the case of $k = q - g$, the thermal conductivity is

$$\kappa_{k=q+g} = \frac{k_B\beta^2\hbar^2}{4V}\sum_q{}' \frac{e^{\beta\hbar\tilde{\omega}_q^{(r)}}}{\big(e^{\beta\hbar\tilde{\omega}_q^{(r)}}-1\big)^2}\frac{v_q v_{q-g}\omega_q^2\omega_{q+g}^2\Delta_q\Delta_{q+g}\big[\big(\frac{\tilde{\omega}_q^{(r)}}{\omega_q}+\frac{\tilde{\omega}_q^{(r)}}{\omega_{q+g}}\big)^2+\big(\frac{(\tilde{\omega}_q^{(r)})^2}{\omega_q\omega_{q+g}}+1\big)^2\big]}{\tilde{\omega}_q^{(r)}\big[\big|\mathrm{Im}\big(\theta_1^{(r)}+\theta_2^{(r)}\big)\big|_{q\to q}+\big|\mathrm{Im}\big(\theta_1^{(r)}+\theta_2^{(r)}\big)\big|_{q\to q+g}\big]}. \tag{3.25}$$

Case 4. $k = q - 2g$.

For this case, $\eta_1^{(r)}$ and $\eta_3^{(r)}$ disappear, similar to $k = q - g$, and $\eta_2^{(r)}$ is

$$\eta_2 = \frac{(\omega_q\omega_{q-2g})^{1/2}}{\omega_{q-g}^2-\omega_{q-2g}^2}(\Delta_{q-g}-\Delta_{q-2g}-i\Gamma_{q-g}+i\Gamma_{q-2g}) \tag{3.26a}$$

for the substitution of subscripts $k \to q-2g, q \to q$, and

$$\eta_2 = \frac{(\omega_q\omega_{q-2g})^{1/2}}{\omega_{q-g}^2-\omega_q^2}(\Delta_{q-g}-\Delta_q-i\Gamma_{q-g}+i\Gamma_q) \tag{3.26b}$$

for substitution of subscripts $k \to q, q \to q-2g$, then we have

$$J_{q-2gq} = -\frac{2}{\pi[\exp(\beta\hbar\omega)-1]}\left\{\frac{\alpha^4\mathrm{Im}\big(\theta_1^{(r)}+\theta_2^{(r)}\big)\mathrm{Re}\big(\eta_2^{(r)}\big)+\alpha^2\big[\omega^2-\big(\tilde{\omega}_q^{(r)}\big)^2\big]\mathrm{Im}\big(\eta_2^{(r)}\big)}{\big[\omega^2-\big(\tilde{\omega}_q^{(r)}\big)^2\big]^2+\alpha^4\big[\mathrm{Im}\big(\theta_1^{(r)}+\theta_2^{(r)}\big)\big]^2}\right\}_{k\to q-2g, q\to q}, \tag{3.27a}$$

$$J_{qq-2g} = -\frac{2}{\pi[\exp(\beta\hbar\omega)-1]}\left\{\frac{\alpha^4\mathrm{Im}\big(\theta_1^{(r)}+\theta_2^{(r)}\big)\mathrm{Re}\big(\eta_2^{(r)}\big)+\alpha^2\big[\omega^2-\big(\tilde{\omega}_q^{(r)}\big)^2\big]\mathrm{Im}\big(\eta_2^{(r)}\big)}{\big[\omega^2-\big(\tilde{\omega}_q^{(r)}\big)^2\big]^2+\alpha^4\big[\mathrm{Im}\big(\theta_1^{(r)}+\theta_2^{(r)}\big)\big]^2}\right\}_{k\to q, q\to q-2g}. \tag{3.27b}$$

The thermal conductivity is

$$\begin{aligned}\kappa_{k=q-2g} = {}& \frac{k_B\beta^2\hbar^2\alpha^2}{4V}\sum_q{}' v_q v_{q-2g}\omega_q^2\omega_{q-2g}^2\frac{e^{\beta\hbar\tilde{\omega}_q^{(r)}}}{\big(e^{\beta\hbar\tilde{\omega}_q^{(r)}}-1\big)^2}\\ &\times\frac{(\Delta_{q-g}-\Delta_q)(\Delta_{q-g}-\Delta_{q-2g})\big[\big(\frac{\tilde{\omega}_q^{(r)}}{\omega_q}+\frac{\tilde{\omega}_q^{(r)}}{\omega_{q-2g}}\big)^2+\big(\frac{(\tilde{\omega}_q^{(r)})^2}{\omega_q\omega_{q-2g}}+1\big)^2\big]}{\tilde{\omega}_q^{(r)}\big(\omega_{q-g}^2-\omega_{q-2g}^2\big)\big(\omega_{q-g}^2-\omega_q^2\big)\big[\big|\mathrm{Im}\big(\theta_1^{(r)}+\theta_2^{(r)}\big)\big|_{q\to q}+\big|\mathrm{Im}\big(\theta_1^{(r)}+\theta_2^{(r)}\big)\big|_{q\to q-2g}\big]}.\end{aligned} \tag{3.28}$$

Case 5. $k = q + 2g$,

$$\kappa_{k=q+2g} = \frac{k_B\beta^2\hbar^2\alpha^2}{4V}\sum_q{}' v_q v_{q+2g}\omega_q^2\omega_{q+2g}^2 \frac{e^{\beta\hbar\tilde{\omega}_q^{(r)}}}{\big(e^{\beta\hbar\tilde{\omega}_q^{(r)}}-1\big)^2} \times \frac{(\Delta_{q+g}-\Delta_q)(\Delta_{q+g}-\Delta_{q+2g})\big[\big(\frac{\tilde{\omega}_q^{(r)}}{\omega_q}+\frac{\tilde{\omega}_q^{(r)}}{\omega_{q+2g}}\big)^2+\big(\frac{(\tilde{\omega}_q^{(r)})^2}{\omega_q\omega_{q+2g}}+1\big)^2\big]}{\tilde{\omega}_q^{(r)}\big(\omega_{q+g}^2-\omega_{q+2g}^2\big)\big(\omega_{q+g}^2-\omega_q^2\big)\big[\big|\mathrm{Im}\big(\theta_1^{(r)}+\theta_2^{(r)}\big)\big|_{q\to q}+\big|\mathrm{Im}\big(\theta_1^{(r)}+\theta_2^{(r)}\big)\big|_{q\to q+2g}\big]}. \tag{3.29}$$

The prime symbol in Eqs. (3.24), (3.25), (3.28), and (3.29) represents a similar meaning as in Eqs. (3.13) and (3.14). In the current approximation, we can obtain a series representation of the resonance frequency of scattering phonons. It is evident from the reciprocal of the phonon's lifetime. As an example, we inspect Eq. (3.21). The phonon lifetime has

$$\tau^{-1} \propto \frac{\alpha^2\tilde{\omega}_q^{(r)}}{\omega_q^2}\big|\mathrm{Im}\big(\theta_1^{(r)}+\theta_2^{(r)}\big)\big| = \frac{\alpha^2\tilde{\omega}_q^{(r)}}{\omega_q^2}\left|-\Gamma_{q-g}-\Gamma_{q+g}+\big[\big(\tilde{\omega}_q^{(r)}\big)^2-\omega_q^2\big]\sum_{s=1}^{n-2}\frac{\Gamma_{q+(s+1)g}-\Gamma_{q+sg}}{\omega_{q+sg}^2-\omega_{q+(s+1)g}^2}\right|, \tag{3.30}$$

where $\Gamma_{q+sg} = \pi\delta[(\tilde{\omega}_q^{(r)})^2-\omega_{q+sg}^2]$. The formula reveals that a phonon will be scattered resonantly when the frequency of the phonon satisfies the condition,

$$\tilde{\omega}_q^{(r)} = |\omega_{q+sg}|, \tag{3.31}$$

where s is any integer. The resonance frequency number n satisfies the condition that ns_r is the smallest integer.

E. $a = s_i b$

Here, s_i is an irrational number, and our system is an incommensurate state. $g = \frac{2\pi s_i}{a}$. Any integer multiple of g is not a reciprocal lattice vector. The spectral-density function is

$$J_{kq} = -\frac{2}{\pi[\exp(\beta\hbar\omega)-1]}\frac{\alpha^2\mathrm{Im}\big(\theta_1^{(i)}+\theta_2^{(i)}\big)\big\{\delta_{qk}\omega_q+\mathrm{Re}\big[\alpha\eta_1^{(i)}+\alpha^2\big(\eta_2^{(i)}-\eta_3^{(i)}\big)\big]\big\}+\big[\omega^2-\big(\tilde{\omega}_q^{(i)}\big)^2\big]\mathrm{Im}\big[\alpha\eta_1^{(i)}+\alpha^2\big(\eta_2^{(i)}-\eta_3^{(i)}\big)\big]}{\big[\omega^2-\big(\tilde{\omega}_q^{(i)}\big)^2\big]^2+\alpha^4\big[\mathrm{Im}\big(\theta_1^{(i)}+\theta_2^{(i)}\big)\big]^2}, \tag{3.32}$$

where $\tilde{\omega}_q^{(i)}, \alpha, \theta_1^{(i)}, \theta_2^{(i)}, \eta_1^{(i)}, \eta_2^{(i)}$, and $\eta_3^{(i)}$ are defined in paper I. From the spectral-density function and similar to the commensurate state in Sec. III D, the thermal conductivity of the lattice is

Case 1. $k = q$,

$$\kappa_{k=q} = \frac{k_B\beta^2\hbar^2}{8V\alpha^2}\sum_q\frac{e^{\beta\hbar\tilde{\omega}_q^{(i)}}}{\big(e^{\beta\hbar\tilde{\omega}_q^{(i)}}-1\big)^2}\left[1+6\left(\frac{\tilde{\omega}_q^{(i)}}{\omega_q}\right)^2+\left(\frac{\tilde{\omega}_q^{(i)}}{\omega_q}\right)^4\right]\frac{v_q^2\omega_q^4}{\tilde{\omega}_q^{(i)}}\frac{\big(1-\frac{\alpha^2}{\omega_q}\mathrm{Re}\,\eta_3^{(i)}\big)^2}{\big|\mathrm{Im}\big(\theta_1^{(i)}+\theta_2^{(i)}\big)\big|}. \tag{3.33}$$

Case 2. $k = q - g$,

$$\kappa_{k=q-g} = \frac{k_B\beta^2\hbar^2}{4V}\sum_q{}'\frac{e^{\beta\hbar\tilde{\omega}_q^{(i)}}}{\big(e^{\beta\hbar\tilde{\omega}_q^{(i)}}-1\big)^2}\frac{v_q v_{q-g}\omega_q^2\omega_{q-g}^2\Delta_q\Delta_{q-g}\big[\big(\frac{\tilde{\omega}_q^{(i)}}{\omega_q}+\frac{\tilde{\omega}_q^{(i)}}{\omega_{q-g}}\big)^2+\big(\frac{(\tilde{\omega}_q^{(i)})^2}{\omega_q\omega_{q-g}}+1\big)^2\big]}{\tilde{\omega}_q^{(i)}\big[\big|\mathrm{Im}\big(\theta_1^{(i)}+\theta_2^{(i)}\big)\big|_{q\to q}+\big|\mathrm{Im}\big(\theta_1^{(i)}+\theta_2^{(i)}\big)\big|_{q\to q-g}\big]}. \tag{3.34}$$

Case 3. $k = q + g$,

$$\kappa_{k=q+g} = \frac{k_B\beta^2\hbar^2}{4V}\sum_q{}'\frac{e^{\beta\hbar\tilde{\omega}_q^{(i)}}}{\big(e^{\beta\hbar\tilde{\omega}_q^{(i)}}-1\big)^2}\frac{v_q v_{q-g}\omega_q^2\omega_{q+g}^2\Delta_q\Delta_{q+g}\big[\big(\frac{\tilde{\omega}_q^{(i)}}{\omega_q}+\frac{\tilde{\omega}_q^{(i)}}{\omega_{q+g}}\big)^2+\big(\frac{(\tilde{\omega}_q^{(i)})^2}{\omega_q\omega_{q+g}}+1\big)^2\big]}{\tilde{\omega}_q^{(i)}\big[\big|\mathrm{Im}\big(\theta_1^{(i)}+\theta_2^{(i)}\big)\big|_{q\to q}+\big|\mathrm{Im}\big(\theta_1^{(i)}+\theta_2^{(i)}\big)\big|_{q\to q+g}\big]}. \tag{3.35}$$

Case 4. $k = q - 2g$,

$$\kappa_{k=q-2g} = \frac{k_B\beta^2\hbar^2\alpha^2}{4V}\sum_q{}' v_q v_{q-2g}\omega_q^2\omega_{q-2g}^2 \frac{e^{\beta\hbar\tilde{\omega}_q^{(i)}}}{\big(e^{\beta\hbar\tilde{\omega}_q^{(i)}}-1\big)^2} \times \frac{(\Delta_{q-g}-\Delta_q)(\Delta_{q-g}-\Delta_{q-2g})\big[\big(\frac{\tilde{\omega}_q^{(i)}}{\omega_q}+\frac{\tilde{\omega}_q^{(i)}}{\omega_{q-2g}}\big)^2+\big(\frac{(\tilde{\omega}_q^{(i)})^2}{\omega_q\omega_{q-2g}}+1\big)^2\big]}{\tilde{\omega}_q^{(i)}\big(\omega_{q-g}^2-\omega_{q-2g}^2\big)\big(\omega_{q-g}^2-\omega_q^2\big)\big[\big|\mathrm{Im}\big(\theta_1^{(i)}+\theta_2^{(i)}\big)\big|_{q\to q}+\big|\mathrm{Im}\big(\theta_1^{(i)}+\theta_2^{(i)}\big)\big|_{q\to q-2g}\big]}. \tag{3.36}$$

Case 5. $k = q + 2g$,

$$\kappa_{k=q+2g} = \frac{k_B\beta^2\hbar^2\alpha^2}{4V}\sum_q{}' v_q v_{q+2g}\omega_q^2\omega_{q+2g}^2 \frac{e^{\beta\hbar\tilde{\omega}_q^{(i)}}}{\big(e^{\beta\hbar\tilde{\omega}_q^{(i)}}-1\big)^2} \times \frac{(\Delta_{q+g}-\Delta_q)(\Delta_{q+g}-\Delta_{q+2g})\Big[\Big(\frac{\tilde{\omega}_q^{(i)}}{\omega_q}+\frac{\tilde{\omega}_q^{(i)}}{\omega_{q+2g}}\Big)^2+\Big(\frac{(\tilde{\omega}_q^{(i)})^2}{\omega_q\omega_{q+2g}}+1\Big)^2\Big]}{\tilde{\omega}_q^{(i)}\big(\omega_{q+g}^2-\omega_{q+2g}^2\big)\big(\omega_{q+g}^2-\omega_q^2\big)\Big[\big|\mathrm{Im}\big(\theta_1^{(i)}+\theta_2^{(i)}\big)\big|_{q\to q}+\big|\mathrm{Im}\big(\theta_1^{(i)}+\theta_2^{(i)}\big)\big|_{q\to q+2g}\Big]}. \quad (3.37)$$

Similar to the behavior of an incommensurate state of any order, an irrational s_i in principle will lead to infinite resonance frequencies. These frequencies satisfy

$$\tilde{\omega}_q^{(i)} = |\omega_{q+sg}|, \quad (3.38)$$

where s is any integer.

IV. DISCUSSIONS

Fundamental to the usefulness of complex thermoelectric materials is the need to optimize a variety of conflicting properties. Maximizing a material's thermoelectric figure of merit requires high electrical conductivity and low thermal conductivity [7]. One method for circumventing the inherent conflict of these two requirements is to imagine a complex material with distinct regions, each providing different functions. The layered structure may have regions composed of a high-mobility semiconductor that assures high electrical conductivity, interwoven with a region of low thermal conductivity. Layered cobaltite oxides, such as Na_xCoO_2 [3], $(Ca_2CoO_3)_{0.62}CoO_2$ [4,8], and $Bi_{2-x}Pb_xSr_2Co_2O_y$ [6], may have a CoO_2 layer with high electrical conductivity and neighboring layers with low lattice thermal conductivity. The lattice periods of the two interpenetrating layers generally are incommensurate along a lattice direction. The FK model can describe well the phonon properties of a layered structure with different lattice periods. Therefore, our theoretical results can explain the low thermal conductivity of the lattice in layered materials.

According to our theoretical calculations, the FK on-site potential causes two extra mechanisms of phonon scattering: resonance and anharmonic scattering (other scattering mechanisms, such as point impurities, three-phonon processes, and boundary scattering, are present in almost all crystals). We note that the anharmonic scattering of the FK model differs from that of the anharmonic potential in general crystals. To distinguish the difference, hereafter, we consider the anharmonic scattering of the FK model as anharmonic scattering and the anharmonic scattering of general crystals as three-phonon processes. Resonance scattering is a discrete process. The number of resonance frequencies depends on the ratio between the period of the unperturbed lattice and the perturbation caused by the FK on-site potential. The number becomes infinite when the ratio is irrational. The phonons' lifetime for resonance scattering is zero, i.e., these phonons are localized completely. The anharmonic scattering from the cubic term of the FK on-site potential expansion exists only for those states higher than second-order commensurate ones. The anharmonic scattering will scatter phonons of all frequencies, and then the phonon's lifetime has a nonzero value. These two mechanisms mainly will determine the lattice thermal conductivity for this kind of material. In the following, we discuss them separately.

A. Anharmonic scattering

Anharmonic phonon scattering comes mainly from the cubic term $C_3(k_1,k_2,k_3)$ (see paper I) of the expansion of the FK on-site potential. As mentioned in paper I, the calculation due to adding $C_3(k_1,k_2,k_3)$ will become very complex so that it is very difficult to analytically estimate the effect of $C_3(k_1,k_2,k_3)$ for a structure higher than a three-order commensurate one. However, some useful conclusions can be obtained when we carefully inspect the calculated results [including the coefficient α_3 terms of Eq. (S.60) in the Supplemental Material of paper I] in the third-order commensurate lattices. From Eq. (S.60), a direct method to reduce the thermal conductivity is attained by raising the coefficient α_3 of the cubic term, i.e., the amplitude V_0 of the FK on-site potential. This resolution is consistent with the results of the simulation of Tsironis *et al.* [16]. In addition, the second and third terms of Eq. (S.60) include $\Gamma_{q+(2\pi/\beta a)}$ and $\Gamma_{q-(2\pi/\beta a)}$, implying that the $C_3(k_1,k_2,k_3)$ term also can lead to resonance scattering. Resonance scattering is discussed later because it also is caused by $C_2(k_1,k_2)$ and $C_4(k_1,k_2,k_3,k_4)$. Comparing the last six terms in Eq. (S.60) from the FK on-site potential with the expression of three phonon processes in general crystals [20,22], some special three-phonon scattering processes are known. These scattering processes represent the interaction among an incoming phonon with a wave vector k, an outgoing phonon with a wave vector q, and a phonon with a wave vector $\frac{2\pi}{3a}$ or $-\frac{2\pi}{3a}$ that is from the FK on-site potential. It means that the anharmonic scattering processes are similar to general three-phonon scattering, but one of these three phonons in the former has integral multiples of the wave vector of the FK on-site potential. For this potential with $a = \frac{b}{3}$, only the phonons with the wave vectors $\frac{2\pi}{3a}$ and $-\frac{2\pi}{3a}$ are supplied to the anharmonic scattering processes. For a higher-order commensurate state, more phonons will join the anharmonic scattering processes. Theoretically, infinite phonons will join these scattering processes in an incommensurate lattice. From the analysis to the anharmonic scattering, we know that changing the lattice constants of the two interpenetrating sublattices and making the layered structure into a high-order commensurate or incommensurate state is an effective way to obtain a low thermal conductivity.

B. Resonance scattering

Phonon resonance scattering efficiently reduces the lattice thermal conductivity [23]. By fitting the experimental data for thermal conductivity in the layered cobaltite oxides,

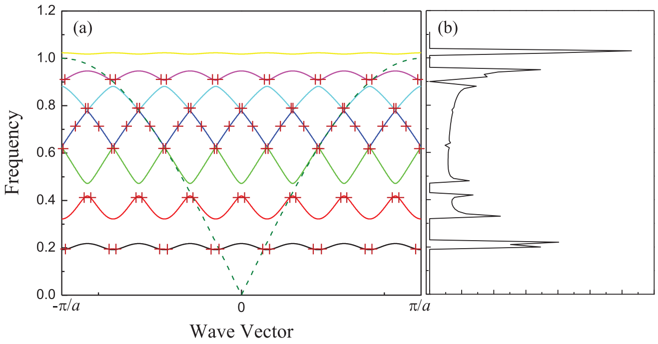

FIG. 2. (Color online) The (a) phonon dispersions and (b) density of states of a commensurate chain with $b = \frac{7}{6}a$, $\omega_L = 1$, and $\frac{\pi^2 V_0}{ma^2} = 0.05$. The dashed line is the dispersion without perturbation. The points showed by dark red addition signs meet $\tilde{\omega}_q^{(r)} = |\omega_{q+sg}|$. The corresponding frequencies of these points are the resonant ones.

we showed previously that the low thermal conductivity in the system mainly results from resonance scattering [8]. Now, our theory further confirms that resonance scattering from the FK on-site potential is an important factor for the lattice thermal conductivity. According to our theory, we can employ two ways to reduce the lattice thermal conductivity in layered materials: (1) increasing the number of resonance frequencies and (2) adjusting the resonance frequencies and letting phonons with that resonance frequency have a density of states as large as possible.

Changing two parameters can achieve both these two goals: (1) Alter the lattice constants of the two interpenetrating sublattices, and (2) change the interaction strength between them, i.e., the amplitude V_0 of the FK on-site potential. Undoubtedly, the change in lattice constant is directly linked to the number of resonance frequencies. When we transfer our system from a commensurate one to an incommensurate one, the number of resonance frequencies increases from a finite number to infinity. However, we emphasize that such a commensurate-incommensurate transition depends on both the interaction strength between the two sublattices and their lattice constants [24]. Changing the strength of the interaction can significantly alter phonon dispersion and the density of states. Figure 2 illustrates phonon dispersion and the density of states of the commensurate state $b = \frac{7}{6}a$ with $\frac{\pi^2 V_0}{ma^2} = 0.05$. Comparing Figs. 4(a) and 4(d) in paper I with Figs. 2(a) and 2(b) clearly illustrates that the changing V_0 not only alters the shape of the dispersion curves of different branches, but also moves their position. These changes, such as that in the density of states with resonance frequency, may be used to adjust lattice thermal conductivity. Figure 2 also depicts the resonance frequencies with various wave vectors (the points of the addition signs). Undoubtedly, the number of the resonance frequencies greatly increases with an increase in the order of commensurate lattice, and the number will be infinity in an incommensurate lattice.

As discussed above, the anharmonic scattering from the FK model is similar to general three-phonon scattering, and it is difficult to obtain an analytical expression of the scattering in any order commensurate structure. Therefore, we do not incorporate the anharmonic scattering from the FK model into our subsequent calculations. In any case, such scattering always will further reduce the lattice thermal conductivity. Resonance scattering can dramatically decrease the lattice thermal conductivity [23,25]. However, thermal conductivity diverges when only the resonance scattering is used to the calculation because phonons with a large deviation from resonance frequency will not be scattered, and then the nonscattering phonons will lead to an infinite thermal conductivity. Similar divergences also occur in calculating the thermal conductivity of high-concentration harmonic isotopically disordered mixed crystals [26] and of the interfacial strain field between dissimilar lattices [27] because phonons with a long wavelength are not scattered by isotopic defects and by the interfacial strain field. The existence of the divergence of resonance scattering in this paper is clearly physical, and it can be removed in real systems by other phonon-scattering mechanisms, such as point defects, boundaries, and three-phonon scattering. As mentioned, the three scattering mechanisms inevitably exist in most real crystals. Therefore, it is necessary to add the three scattering mechanisms in calculating thermal conductivity not only to remove the divergence of resonance scattering, but also to compare it with and without the resonance scattering. All phonon-scattering processes can be combined by frequency-dependent relaxation times [28]. The frequency-dependent relaxation times for scattering by point defects, boundaries, and three-phonon process have been studied widely. Based on Callaway's phenomenological model [28], the combination of these relaxation times is

$$\tau^{-1} = \tau_D^{-1} + \tau_B^{-1} + \tau_P^{-1} + \cdots . \tag{4.1}$$

wherein the first three terms, $\tau_D^{-1} = A\omega^4$, $\tau_B^{-1} = \frac{v}{L}$, and $\tau_P^{-1} = B\omega^2 T\ \exp(-\frac{\theta_D}{3T})$, respectively, come from scattering by point defects, boundaries, and three-phonon processes. The ellipsis in Eq. (4.1) shows any other existing scattering mechanisms. v is the group speed of the phonons, θ_D is the Debye temperature, and L, A, and B, respectively, are the three constants of materials dependent on grain size, the density of point impurities, and the intensity of the anharmonic force constant. In applying Callaway's theory, L, A, and B usually are determined from fitting experimental data.

The lattice thermal conductivity derived from the Kubo formula based on a physical model can reveal details of their basic physical nature. However, to include the three scattering mechanisms in Eq. (4.1) into our calculation, we can rewrite our theoretical derivation using some approximation [26,29]. Comparing our results with Callaway's formula, as an example, the relaxation time per normal mode in the second term of Eq. (3.7) is

$$\tau(q) = \frac{\omega_q \omega_{q+(\pi/a)}\left[\left(\tilde{\omega}_q^{(2)}\right)^2 - \omega_q^2\right]\left[\left(\tilde{\omega}_q^{(2)}\right)^2 - \omega_{q+(\pi/a)^2}\right]}{4M_2^4 \tilde{\omega}_q^{(2)}\left(\Gamma_q + \Gamma_{q+(\pi/a)}\right)} \times \left[\left(1 + \frac{\left(\tilde{\omega}_q^{(2)}\right)^2}{\omega_q \omega_{q+(\pi/a)}}\right)^2 + \left(\frac{\tilde{\omega}_q^{(2)}}{\omega_q} + \frac{\tilde{\omega}_q^{(2)}}{\omega_{q+(\pi/a)}}\right)^2\right]. \tag{4.2}$$

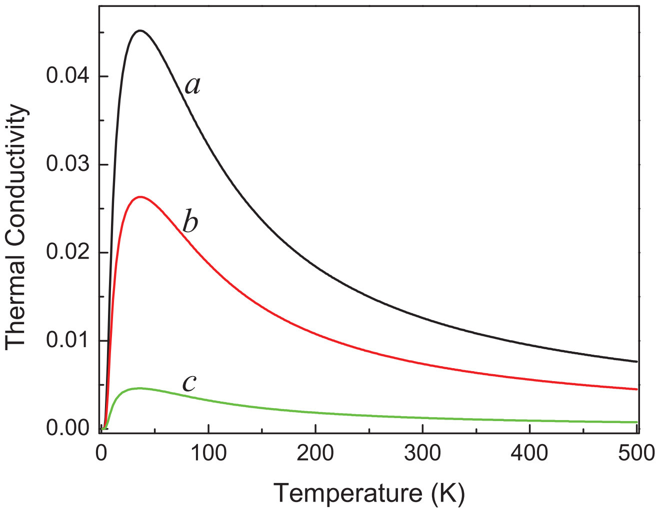

FIG. 3. (Color online) Thermal conductivity (in atomic units) as a function of temperature in three cases: (a) general crystal, (b) commensurate with $b = \frac{7}{6}a$, and (c) incommensurate with $b = 1.17a$. The following parameters were used in the calculation:$\omega_L = 10^{13}$ Hz; $L = 1\ \mu$m; $A = 10^{-41}$ s^3; $B = 5 \times 10^{-18}$ s/K; $v = 3000$ m/s; $\theta_D =$ 270 K.

The second term of Eq. (3.7) becomes

$$\kappa = \sum_q \tau(q)C(q)v_q^2, \qquad (4.3)$$

where $C(q) = \frac{k_B\beta^2\hbar^2\omega_q\omega_{q+(\pi/a)}e^{\beta\hbar\tilde{\omega}_q^{(2)}}}{(e^{\beta\hbar\tilde{\omega}_q^{(2)}}-1)^2}$ has the unit of the phonon specific heat, and it can be termed the effective phonon specific heat. Equation (4.3) is same as the form of Callaway's theory [28]. Thereafter, we can group all the scattering mechanisms into Callaway's phenomenological model. In our calculations, the relaxation times of the resonance scattering from the FK model will be obtained from the results of Sec. III, whereas the total relaxation time is calculated from Eq. (4.1). The lattice thermal conductivities of the three structures, general crystal, commensurate and incommensurate ones, were calculated, and the results are shown in Fig. 3. The black line (curve a) represents the findings for the point impurities, boundary scattering, and three-phonon processes [28]. The red line (curve b) and the green line (curve c) show the thermal conductivities added by resonance scattering of the commensurate structure with $b = \frac{7}{6}a$ and the incommensurate structure with $b = 1.17a$, respectively. In calculating these curves, we let resonance scattering occur with $|\frac{\tilde{\omega}_q^{(r)}-\omega_{q+sg}}{\tilde{\omega}_q^{(r)}}| <$ 0.01. Figure 3 shows that the thermal conductivity of an incommensurate structure with $b = 1.17a$ is almost one order of magnitude lower than that of the general crystal. It can explain the low lattice thermal conductivity that occurs in materials consisting of two interpenetrating incommensurate sublattices.

V. SUMMARY AND CONCLUSIONS

We studied the lattice thermal conductivity resulting from the FK model, beginning first with several low-order commensurate states. The first-order commensurate state, i.e., the period of the unperturbed lattice is same as that of the FK on-site potential and has infinite lattice thermal conductivity in our approximation. The higher-than-first-order commensurate states will have resonance scattering for some special frequencies. In addition to resonance scattering, we identified anharmonic scattering resulting from the cubic term of the expansion of the FK on-site potential in those states higher than second-order commensurate ones. The number of the resonance frequencies depends on the ratio between the period of the unperturbed lattice and that of the FK on-site potential. Their number becomes infinite when the ratio is irrational. The change in amplitude of the FK on-site potential can alter the intensity of anharmonic scattering and the resonance frequency. If the phonon with resonance frequency has a density of states as large as possible, it is very useful in reducing the lattice thermal conductivity in the layered materials. Our theoretical results can be used to develop strategies to lower the lattice's thermal conductivity in actual layered thermoelectric materials.

ACKNOWLEDGMENTS

The work was supported by the U.S. Department of Energy, Office of Basic Energy Science, Materials Science and Engineering Division, under Contract No. DE-AC02-98CH10886.

---

[1] Q. Meng, L. Wu, D. O. Welch, and Y. Zhu, Lattice vibrations in the Frenkel-Kontorova model. I. Phonon dispersion, number density, and energy, preceding paper, Phys. Rev. B **91**, 224305 (2015).

[2] O. M. Braun and Y. S. Kivshar, *The Frenkel-Kontorova Model, Concept, Method and Application* (Springer-Verlag, Berlin/Heidelberg/New York, 2004).

[3] I. Terasaki, Y. Sasago, and K. Uchinokura, Large thermoelectric power in $NaCo_2O_4$ single crystals, Phys. Rev. B **56**, R12685 (1997).

[4] M. Shikano and R. Funahashi, Electrical and thermal properties of single-crystalline $(Ca_2CoO_3)_{0.7}CoO_2$ with a $Ca_3Co_4O_9$ structure, Appl. Phys. Lett. **82**, 1851 (2005).

[5] A. Satake, H. Tanaka, T. Ohkawa, T. Fujii, and I. Terasaki, Thermal conductivity of the thermoelectric layered cobalt oxides measured by the Harman method, J. Appl. Phys. **96**, 931 (2004).

[6] I. Terasaki, H. Tanaka, A. Satake, S. Okada, and T. Fujii, Out-of-plane thermal conductivity of the layered thermoelectric oxide $Bi_{2-x}Pb_xSr_2Co_2O_y$, Phys. Rev. B **70**, 214106 (2004).

[7] G. J. Snyder and E. S. Toberer, Complex thermoelectric materials, Nature Mater. **7**, 105 (2008).

[8] L. Wu, Q. Meng, C. Jooss, J.-C. Zheng, H. Inada, D. Su, Q. Li, and Y. Zhu, Origin of phonon glass-electron crystal behavior in thermoelectric layered cobaltate, Adv. Funct. Mater. **23**, 5728 (2013).

[9] M. J. Gillan and R. W. Holloway, Transport in the Frenkel-Kontorova model. III. Thermal conductivity, J. Phys. C: Solid State Phys. **18**, 5705 (1985).

[10] H. Kaburaki and M. Machida, Thermal conductivity in one-dimensional lattices of Fermi-Pasta-Ulam type, Phys. Lett. A **181**, 85 (1993)

[11] S. Lepri, R. Livi, and A. Politi, Heat conduction in chains of nonlinear oscillators, Phys. Rev. Lett. **78**, 1896 (1997).

[12] S. Lepri, R. Livi, and A. Politi, On the anomalous thermal conductivity of one-dimensional lattices, Europhys. Lett. **43**, 271 (1998).

[13] T. Hatano, Heat conduction in the diatomic Toda lattice revisited, Phys. Rev. E **59**, R1 (1999).

[14] B. Hu, B. Li, and H. Zhao, Heat conduction in one-dimensional nonintegrable systems, Phys. Rev. E **61**, 3828 (2000).

[15] B. Li, H. Zhao, and B. Hu, Can disorder induce a finite thermal conductivity in 1D lattices?, Phys. Rev. Lett. **86**, 63 (2001).

[16] G. P. Tsironis, A. R. Bishop, A. V. Savin, and A. V. Zolotaryuk, Dependence of thermal conductivity on discrete breathers in lattices, Phys. Rev. E **60**, 6610 (1999).

[17] A. V. Savin and O. V. Gendelman, Heat conduction in one-dimensional lattices with on-site potential, Phys. Rev. E **67**, 041205 (2003).

[18] R. J. Hardy, Energy-flux operator for a lattice, Phys. Rev. **132**, 168 (1963).

[19] D. N. Zubarev, Double-time green functions in statistical physics, Sov. Phys. Usp. **3**, 320 (1960).

[20] A. A. Maradudin and A. E. Fein, Scattering of neutrons by an anharmonic crystal, Phys. Rev. **128**, 2589 (1962).

[21] B. V. Thompson, Neutron scattering by an anharmonic crystal, Phys. Rev. **131**, 1420 (1963).

[22] K. N. Pathak, Theory of anharmonic crystals, Phys. Rev. **139**, A1569 (1965).

[23] R. O. Pohl, Thermal conductivity and phonon resonance scattering , Phys. Rev. Lett. **8**, 481 (1962).

[24] G. Theodorou and T. M. Rice, Statics and dynamics of incommensurate lattices, Phys. Rev. B **18**, 2840 (1978).

[25] P. W. Anderson, B. I. Helperin, and C. M. Varma, Anomalous low-temperature thermal properties of glasses and spin glasses, Philos. Mag. **25**, 1 (1972)

[26] J. K. Flicker and P. L. Leath, Lattice thermal conductivity in high-concentration mixed crystals, Phys. Rev. B **7**, 2296 (1973).

[27] Q. Meng, L. Wu, and Y. Zhu, Phonon scattering of interfacial strain field between dissimilar lattices, Phys. Rev. B **87**, 064102 (2013).

[28] J. Callaway, Model for lattice thermal conductivity at low temperatures, Phys. Rev. **113**, 1046 (1959).

[29] B. Deo and S. N. Behera, Calculation of thermal conductivity by the Kubo formula, Phys. Rev. **141**, 738 (1966).